Virucidal and antiviral activity of astodrimer sodium against SARS-CoV-2 in vitro

Jeremy Paull (jeremy.paull@starpharma.com)
Starpharma Pty Ltd https://orcid.org/0000-0002-9981-421X
Graham Heery
Starpharma Pty Ltd
Michael Bobardt
The Scripps Research Institute
Alex Castellarnau
Starpharma Pty Ltd
Carolyn Luscombe
Starpharma Pty Ltd
Jacinth Fairley
Starpharma Pty Ltd
Philippe Gallay
The Scripps Research Institute

Research Article

Keywords: Astodrimer, COVID-19, dendrimer, antiviral, SARS CoV 2, SPL7013

Posted Date: April 20th, 2021

DOI: https://doi.org/10.21203/rs.3.rs-440941/v1

Version of Record: A version of this preprint was published at Antiviral Research on May 16th, 2021. See the published version at https://doi.org/10.1016/j.antiviral.2021.105089.

Title: Virucidal and antiviral activity of astodrimer sodium against SARS-CoV-2 *in vitro.*

Authors: Jeremy R.A. Paull[a,*]; Graham P. Heery [a], Michael D. Bobardt[b], Alex Castellarnau[a]; Carolyn A. Luscombe[a]; Jacinth K. Fairley[a]; Philippe A. Gallay[b]

Author affiliations:

[a] Starpharma Pty Ltd, 4-6 Southampton Crescent, Abbotsford, Victoria 3067, Australia

[b] Department of Immunology and Microbiology, The Scripps Research Institute, La Jolla, CA 92307, USA

* Corresponding author: jeremy.paull@starpharma.com (JP)

Declaration of interest:

The authors declare the following financial interests that may be considered as potential competing interests: J.R.A.P., J.K.F. and G.P.H. are paid employees of Starpharma Pty Ltd. A.C. and C.A.L. are paid consultants to Starpharma Pty Ltd.

Word count:

Abstract: 284

Text: 3463

Inserts: 4 tables, 5 figures

Abstract

An effective response to the ongoing coronavirus disease (COVID-19) pandemic caused by severe acute respiratory syndrome coronavirus 2 (SARS-CoV-2) will involve a range of complementary preventive modalities. The current studies were conducted to evaluate the *in vitro* SARS-CoV-2 antiviral and virucidal activity of astodrimer sodium, a dendrimer with broad spectrum antimicrobial activity, including against enveloped viruses in *in vitro* and *in vivo* models, that is marketed for antiviral and antibacterial applications. We report that astodrimer sodium inhibits replication of SARS-CoV-2 in Vero E6 and Calu-3 cells, with 50% effective concentrations (EC_{50}) for i) reducing virus-induced cytopathic effect of 0.002 to 0.012 mg/mL in Vero E6 cells, and ii) infectious virus release by plaque assay of 0.019 to 0.032 mg/mL in Vero E6 cells and 0.031 to 0.037 mg/mL in Calu-3 cells. The selectivity index (SI) in these assays was as high as 2197. Astodrimer sodium was also virucidal, reducing SARS-CoV-2 infectivity by >99.9% (>3 $\log_{10}$) within 1 minute of exposure, and up to >99.999% (>5 $\log_{10}$) shown at astodrimer sodium concentrations of 10 to 30 mg/mL in Vero E6 and Calu-3 cell lines. Astodrimer sodium also inhibited infection in a primary human airway epithelial cell line. The data were similar for all investigations and were consistent with the potent antiviral and virucidal activity of astodrimer sodium being due to inhibition of virus-host cell interactions, as previously demonstrated for other viruses. Further studies will confirm if astodrimer sodium binds to SARS-CoV-2 spike protein and physically blocks initial attachment of the virus to the host cell. Given the *in vitro* effectiveness and significantly high SI, astodrimer sodium warrants further investigation for potential as a nasally administered or inhaled antiviral agent for SARS-CoV-2 prevention and treatment applications.

Keywords: Astodrimer; COVID-19; dendrimer; antiviral; SARS-CoV-2; SPL7013

1. Introduction

The ongoing pandemic coronavirus disease 2019 (COVID-19), caused by severe acute respiratory syndrome coronavirus-2 (SARS-CoV-2) infection, has resulted in unprecedented efforts to rapidly develop strategies to contain infection rates for the protection of vulnerable populations. An effective public health response to the current pandemic will involve currently available vaccines being complemented by supplementary preventive modalities.

SARS-CoV-2 receptors and coreceptors have been shown to be highly expressed in nasal epithelial cells (Sungnak et al., 2020). This finding is consistent with the virus infectivity or replication pattern along the respiratory tract, which peaks proximally (nasal cavity) and is relatively minimal in the distal alveolar regions (Hou et al., 2020). These findings suggest that nasal carriage of the virus is a key feature of transmission, and that nasally administered therapeutic modalities could be potentially effective in helping to prevent spread of infection.

Astodrimer sodium (SPL7013) is a generation-four lysine dendrimer with a polyanionic surface charge (McCarthy et al., 2005) that is active against several enveloped and non-enveloped viruses including human immunodeficiency virus-1 (HIV-1) (Lackman-Smith et al., 2008, Tyssen et al., 2010), herpes simplex virus (HSV)-1 and -2 (Gong et al., 2005), H1N1 and H3N2 influenza virus, human respiratory syncytial virus (HRSV), human papillomavirus (HPV), adenovirus and Zika virus (unpublished data). Astodrimer sodium also has antibacterial properties. Both size and surface charge contribute to the function of the compound (Tyssen et al., 2010), and when administered topically, astodrimer sodium is not absorbed systemically (Chen et al., 2009; O'Loughlin et al., 2010; McGowan et al., 2011).

Vaginally administered astodrimer sodium protected macaques from infection with chimeric simian-HIV-1 (SHIV)$_{89.6P}$ (Jiang et al., 2005), and mice and guinea pigs from HSV-2 infection (Bernstein et al., 2003) in vaginal infection challenge models. Astodrimer 1% Gel (10 mg/mL astodrimer sodium) administered vaginally has been shown to be safe and effective in phase 2 and large phase 3 trials for treatment and prevention of bacterial vaginosis (BV) (Chavoustie et al., 2020; Waldbaum et al., 2020; Schwebke et al., 2021) and is marketed in Europe, Australia, New Zealand and several countries in Asia.

The current studies were conducted to assess the antiviral and virucidal activity of astodrimer sodium against SARS-CoV-2 *in vitro*, to determine its potential as a reformulated, nasally administered or inhaled antiviral agent to help prevent spread of SARS-CoV-2 infection.

2. Materials and methods

2.1 Virus, cell culture, astodrimer sodium and controls

SARS-CoV-2 hCoV-19/Australia/VIC01/2020 was a gift from Melbourne's Peter Doherty Institute for Infection and Immunity (Melbourne, Australia). Virus stock was generated at 360Biolabs (Melbourne, Australia) by two passages in Vero cells in virus growth media, which comprised Minimal Essential Medium (MEM) without L-glutamine supplemented with 1% (w/v) L-glutamine, 1.0 µg/mL of L-(tosylamido-2-phenyl) ethyl chloromethyl ketone (TPCK)-treated trypsin (Worthington Biochemical, NJ, USA), 0.2% bovine serum albumin (BSA) and 1% insulin-transferrin-selenium (ITS).

SARS-CoV-2 2019-nCoV/USA-WA1/2020 strain was isolated from an oropharyngeal swab from a patient with a respiratory illness who developed clinical disease (COVID-19) in January 2020 in Washington, US, and sourced from BEI Resources (NR-52281). Virus was derived from

88 African green monkey kidney Vero E6 cells or lung homogenates from human angiotensin
89 converting enzyme 2 (hACE2) transgenic mice.

90 Vero E6 and human Calu-3 cell lines were cultured in MEM without L-glutamine supplemented
91 with 10% (v/v) heat-inactivated fetal bovine serum (FBS) and 1% (w/v) L-glutamine. Vero E6
92 and Calu-3 cells were passaged for a maximum of 10 passages for antiviral and virucidal studies.
93 Hank's balanced salt solution (HBSS) with 2% FBS was used for infection. The 2019-
94 nCoV/USA-WA1/2020 strain antiviral assays were performed with a multiplicity of infection
95 (MOI) of 0.1.

96 The virus inoculums for virucidal assays were 10^4, 10^5, and 10^6 pfu/mL. After defined incubation
97 periods, the solution was pelleted through a 20% sucrose cushion (Beckman SW40 Ti rotor) and
98 resuspended in 1.5 mL MEM, which was then added to $2.5x10^4$ cells/well.

99 Primary human bronchial epithelial cells (HBEpC) (Sigma-Aldrich, MO, USA) were grown and
100 maintained in HBEpC/HTEpC growth medium (Cell Applications, CA, USA). These primary
101 cells express the ACE2 receptor and are permissive to SARS-CoV-2 infection. These cells were
102 used to determine the antiviral effect of astodrimer sodium against SARS-CoV-2 in a primary
103 human airway epithelial cell line. Cells were infected with SARS-CoV-2 2019-nCoV/USA-
104 WA1/2020 at 10^3 pfu/mL with 1 mL added to $2.5x10^4$ cells/well. The positive control was
105 addition of 10 μg/mL of SARS-CoV-2 spike protein antibody (pAb, T01KHuRb)
106 (ThermoFisher, MA, USA) at the time of infection.

107 Astodrimer sodium was prepared as 100 mg/mL in water and stored at 4°C. Astodrimer sodium
108 has a molecular weight of 16581.57 g/mol and the structure is described and illustrated in Tyssen

et al., 2010. The purity of the compound used in these studies was assessed by ultra-high-performance liquid chromatography (UPLC) to be 98.79%.

Remdesivir (MedChemExpress, NJ, USA) was used as a positive control in the virus-induced cytopathic effect (CPE) inhibition and plaque assays.

Iota-carrageenan (Sigma-Aldrich, MO, USA) was used in the primary epithelial cell nucleocapsid and plaque assays to compare the antiviral activity of this substance with astodrimer sodium. Concentrations used are those reported to show activity against SARS-CoV-2 (Bansal et al., 2020).

2.2 Virus-induced cytopathic effect inhibition assay

Vero E6 (ATCC-CRL1586) cell stocks were generated in cell growth medium, which comprised MEM without L-glutamine supplemented with 10% (v/v) heat-inactivated FBS and 1% (w/v) L-glutamine. Vero E6 cell monolayers were seeded in 96-well plates at $2x10^4$ cells/well in 100 µL growth medium (MEM supplemented with 1% (w/v) L-glutamine, 2% FBS) and incubated overnight at 37°C in 5% CO_2. SARS-CoV-2 infection was established by using an MOI of 0.05 to infect cell monolayers.

Astodrimer sodium or remdesivir were serially diluted 1:3, 9 times and each compound concentration was assessed for both antiviral efficacy and cytotoxicity in triplicate. Astodrimer sodium was added to Vero E6 cells 1 hour prior to infection or 1 hour post-infection with SARS-CoV-2. Cell cultures were incubated at 37°C in 5% CO_2 for 4 days prior to assessment of CPE. The virus growth media was MEM supplemented with 1% (w/v) L-glutamine, 2% FBS, and 4 µg/mL TPCK-treated trypsin. On Day 4, viral-induced CPE and cytotoxicity of the compound were determined by measuring the viable cells using the

methylthiazolyldiphenyl-tetrazolium bromide (MTT) assay (MP Biomedicals, NSW, Australia). Absorbance was measured at 540-650 nm on a plate reader.

2.3 Antiviral plaque assay evaluation and nucleocapsid ELISA

For the antiviral evaluation, astodrimer sodium was added to cells 1 hour prior to, at the time of, and 1 hour after exposing the cells to virus. For both the antiviral and virucidal assays, at 6 hours after infection, cells were washed to remove astodrimer sodium and/or any virus remaining in the supernatant, in such way that a

Following initial infection, cell cultures were incubated and supernatants recovered after 16 hours or 4 days. The amount of virus in the supernatants was determined by plaque assay (plaque forming unit [pfu]) and by nucleocapsid enzyme-linked immunosorbent assay (ELISA). The plaque assay used was as described in van den Worm et al., 2012, utilizing 2% sodium carboxymethyl cellulose overlay, fixation of cells by 4% paraformaldehyde and staining with 0.1% crystal violet. The nucleocapsid ELISA assay was as described by Bioss Antibodies, USA (BSKV0001).

The assessment of astodrimer sodium cytotoxicity occurred on Day 4 by measuring lactate dehydrogenase (LDH) activity in the cytoplasm using an LDH detection kit (Cayman Chemical), with 0.5% saponin used as the positive cytotoxic control.

2.4 Virucidal assay

For the virucidal evaluation, concentrations of astodrimer sodium (0.0046 to 30 mg/mL) were incubated with SARS-CoV-2 2019-nCoV/USA-WA1/2020 for times ranging from 5 seconds to 2 hours. To neutralize the effect of astodrimer sodium, unbound compound was separated from the astodrimer:virus mixture by pelleting the preincubated mixture through a 20% sucrose cushion (Beckman SW40 Ti rotor). The astodrimer sodium-containing supernatant was removed

(i.e., neutralising the effect of SPL7013) and then the pelleted virus was gently resuspended and added to Vero E6 or Calu-3 cell cultures. Virus infection, cell culture and cytotoxicity assessment was as described for the plaque assay described in Section 2.3.

All antiviral and virucidal assays were performed in triplicate, except where indicated in the results.

2.5 Determination of 50% effective concentration (EC_{50}) and cytotoxicity (CC_{50})

The concentration of compound that gives a 50% reduction in viral-induced CPE, infectious virus (pfu/mL), or secreted viral nucleocapsid (EC_{50}) was calculated using the formula of Pauwels et al., 1998.

The concentration of compound that resulted in a 50% reduction in cell viability (CC_{50}) after 4 days of culture was also calculated by the formula of Pauwels et al., 1998.

2.6 Primary Epithelial Cell Assay

Astodrimer sodium (0, 1.1, 3.3 and 10 mg/mL) or iota-carrageenan (0, 6, 60 and 600 µg/mL) were added to HBEpC cells 1 hour prior to infection with SARS-CoV-2. Cells were cultured for 4 days post-infection and the cell supernatant was analysed for the amount of secreted SARS-CoV-2 nucleocapsid by ELISA, and infectious virus was quantitated by plaque assay, as described in Section 2.3.

3. Results

3.1 Virus-induced cytopathic effect inhibition

In two independent virus-induced CPE inhibition assays, astodrimer sodium inhibited SARS-CoV-2 (hCoV-19/Australia/VIC01/2020) replication in Vero E6 cells in a dose dependent

manner (Table 1). Astodrimer sodium inhibited viral replication when added either 1 hour prior to infection, or 1 hour post-infection with SARS-CoV-2.

Astodrimer sodium was initially tested in the range of 0.0013 to 8.63 mg/mL. In the repeat set of assays, astodrimer sodium was tested in the range of 0.0001 to 0.86 mg/mL to help further characterize the lower end of the dose response curve. The effective and cytotoxic concentrations, and selectivity indices from the assays are shown individually and as means in Table 1 for CPE determined readouts.

The selectivity index (SI) for astodrimer sodium against SARS-CoV-2 in the CPE studies ranged from 793 to 2197 for the initial assays where compound was added 1 hour prior to infection and 1 hour after infection, respectively, and was >70 to >80 in the repeat assays, in which cytotoxicity was not observed up to the highest concentration tested (0.86 mg/mL).

The positive control, remdesivir, was also active in the CPE inhibition assay, with a SI of >33.

3.2 Antiviral efficacy

To determine the ability of astodrimer sodium to inhibit globally diverse SARS-CoV-2 strains, the compound was evaluated against the 2019-nCoV/USA-WA1/2020 virus in Vero E6 cells and human Calu-3 cells. Antiviral readouts were based on virological endpoints of infectious virus or viral nucleocapsid released into the supernatant post-infection. As shown in Table 2 and Figures 1 and 2, astodrimer inhibited the 2019-nCoV/USA-WA1/2020 strain with an EC_{50} 0.019 to 0.032 mg/mL and 0.031 to 0.037 mg/mL for infectious virus release as determined by plaque assay in Vero E6 cell for Calu-3 cells, respectively. These data are consistent with the inhibition by astodrimer of the replication of the Australian SARS-CoV-2 isolate *in vitro*. The dose response data for the nucleocapsid released into the supernatant by ELISA were similar to the infectious

virus release data in each cell line (data not shown). The positive control, remdesivir, was also active in the plaque assay.

3.3 Virucidal efficacy

Virucidal assays investigated if astodrimer sodium could reduce viral infectivity by irreversibly inactivating SARS-CoV-2 prior to infection of Vero E6 cells and human airway Calu-3 cells. Following incubation of virus with astodrimer for up to 2 hours and neutralization of astodrimer, the astodrimer-exposed virus was added to cell cultures. After either 16 hours or 96 hours (Day 4), the cell culture supernatant was collected for assessment of progeny viral infectivity as determined by the amount of secreted infectious virus and nucleocapsid. The SARS-CoV-2 replication lifecycle is completed in approximately 8 hours (Ogando et al., 2020) and in these studies, we sampled at 16 hours (2 lifecycles) or Day 4 (12 lifecycles) post-infection.

Enabling a possible 12 rounds of infection, the Day 4 (96 hour) sampling time point identified that exposure of 10^6 pfu/mL SARS-CoV-2 to astodrimer sodium for 1 to 2 hours resulted in a dose-dependent reduction in viral infectivity, with 10 to 30 mg/mL astodrimer sodium achieving up to >99.999% (>5 $\log_{10}$) reduced infectivity in Vero E6 cells and >99.9% (>3 $\log_{10}$) reduced infectivity in Calu-3 cells (data not shown) compared to untreated virus. SARS-CoV-2 infectivity was also reduced by up to >99.999% in Vero E6 cells when the incubation time of astodrimer (10 to 30 mg/mL) with 10^6 pfu/mL virus was reduced to 15 to 30 minutes (data not shown).

Incubation of astodrimer sodium with viral inoculums of 10^4, 10^5 and 10^6 pfu/mL for as little as 5 seconds resulted in evidence of reduced infectivity, with 10 to 15 minutes exposure being sufficient to achieve >99.9% reduction in virus infectivity, and greater reduction achieved with

lower viral inoculum (>99.999%, 10^4 pfu/mL viral inoculum, 10 to 30 mg/mL astodrimer sodium, and 10 to 15 min incubation time) (Table 3, Figure 3).

When assessed 16 hours post-infection of cells with astodrimer-exposed virus, it was found that ≥10 mg/mL astodrimer sodium inactivated >99.9% SARS-CoV-2 (10^4 pfu/mL) within as little as 1 minute of exposure (Table 4, Figure 4).

3.4 Antiviral Efficacy in Primary Human Airway Epithelial Cells

To determine the ability of astodrimer sodium to prevent SARS-CoV-2 infection of primary human epithelial cells, the compound was evaluated against the 2019-nCoV/USA-WA1/2020 strain in HBEpC cell culture. Astodrimer sodium was found to reduce infection of HBEpC primary cells by SARS-CoV-2 by up to 98% vs virus control by nucleocapsid ELISA (Figure 5A), and by up to 95% in the plaque assay (data not shown). In contrast, treatment with iota-carrageenan had minimal antiviral effect against SARS-CoV-2 in this cell line, with the highest concentration tested reducing infection by just 17% by nucleocapsid ELISA (Figure 5B), and just 21% in the plaque assay (data not shown). The maximum level of inhibition with astodrimer sodium was comparable to inhibition achieved with the SARS-CoV-2 spike protein antibody (pAb, T01KHuRb) positive control (see Figure 5A and B).

4. Discussion

Astodrimer sodium demonstrated potent antiviral activity against globally diverse SARS-CoV-2 strains *in vitro*. Antiviral activity was demonstrated by reduction in CPE, release of infectious virus and release of viral nucleocapsid protein. Antiviral activity was demonstrated when astodrimer sodium was added to cells prior to infection of cells and when the compound was

added to cells already exposed to SARS-CoV-2. Irreversible virucidal activity was demonstrated when astodrimer sodium was mixed with virus for as little as 1 minute.

Of note is a significantly high SI for astodrimer sodium in the antiviral assays relative to other antiviral compounds under investigation for SARS-CoV-2 activity (Pizzorno et al., 2020).

Remdesivir was used as the antiviral positive control for the CPE inhibition and antiviral assays and the experimental EC_{50} was consistent with published data generated with a different clinical isolate of SARS-CoV-2 (Wang et al., 2020).

Astodrimer sodium inhibited infection of a human airway primary epithelial cell by SARS-CoV-2, whereas iota-carrageenan, which is a polyanionic compound in marketed nasal spray formulations, failed to provide significant inhibition at concentrations that have previously been shown to reduce SARS-CoV-2 infection in Vero E6 cells (Bansal et al., 2020). The unique structure of astodrimer sodium, a sulphonated, roughly spherical molecule with a core and densely packed branches radiating out from the core, appears to provide potential benefits over other polyanionic compounds such as iota-carrageenan and heparin, which are linear sulphated molecules with a distribution of molecular weight. The authors are not aware of data showing that iota-carrageenan is virucidal, while heparin has demonstrated a lack of irreversible, virucidal interaction with HSV virion components (Ghosh et al., 2009).

The antiviral data are consistent with astodrimer sodium being a potent inhibitor of early events in the virus lifecycle. The virucidal assay data suggest that astodrimer sodium antiviral activity was consistent with the proposed mechanism of action of binding to virus, thereby irreversibly inactivating virus and blocking infection.

The virucidal activity of astodrimer sodium demonstrated that it irreversibly inhibits the early phase of virus infection and replication. These findings suggest potent inhibition of viral attachment, fusion and entry of the virus, which prevents virus replication and release of infectious virus progeny.

Astodrimer sodium has been previously found to be an effective antiviral that exerts its inhibition in the early virus-host receptor recognition interactions (Tyssen et al., 2010; Telwatte et al., 2011), and its potential mechanism of action against SARS-CoV-2 is likely similar to that identified for other pathogens. Astodrimer sodium was found to bind to HIV-1 by strong electrostatic forces to positively charged clusters of highly conserved amino acids on HIV-1 gp120 protein and/or positively charged amino acid regions located between the stems of V1/V2 and V3 loops, which are exposed by conformational changes to gp120 after viral binding to the receptor/co-receptor complex (Tyssen et al., 2010; Connell and Lortat-Jacob, 2013).

Many viruses utilize negatively charged heparan sulfate proteoglycans (HS) on the cell plasma membrane as an initial means to scan the surface of the cell, and to attach in order to chaperone the virus onto the receptor complex prior to viral entry (Sarrazin et al., 2011; Connell and Lortat-Jacob, 2013). The receptor interactions occur in a sequential manner with virus-HS interactions preceding receptor/co-receptor binding, which combined leads to fusion of the viral envelope and the cell membrane.

Data indicate that astodrimer sodium-gp120 interaction may physically block initial HIV-1 association with HS and thereby block the subsequent virus-receptor complex functions. Virucidal studies of astodrimer sodium determined that it did not disrupt the HIV-1 particle or cause the loss of gp120 spike protein from the viral surface (Telwatte et al., 2011).

A report by Liu et al., 2020, described that densely glycosylated trimeric SARS-CoV-2 spike (S) protein subunit S1, which is important for receptor binding, binds to HS. To engage with the ACE2 receptor, the S protein undergoes a hinge-like conformational change that transiently hides or exposes the determinants of receptor binding (Wrapp et al., 2020). Recent studies have identified the binding of heparin to the receptor binding domain (RBD) of S1 resulting in a conformational change to the S protein (Mycroft-West et al., 2020a, b and c). Mutations in the S protein that are distal from the RBD also impact on viral transmission (Walls et al., 2020; Korber et al., 2020; Yuan et al., 2020). Non-RBD polybasic cleavage sites, including S1/S2 loop (Hoffmann et al., 2020a), have been described on SARS-CoV-2 S protein (Qiao and Olvera de la Cruz, 2020) and may also be a site of potential interaction with astodrimer sodium.

SARS-CoV-2 utilizes the ACE2 receptor for viral infection of host cells (Hoffmann et al., 2020b). Human CoV-NL63 also utilizes HS and ACE2 as its cellular receptor complex (Milewska et al., 2014). The importance of HS for viral infectivity was also demonstrated for close genetically related pseudo-typed SARS-CoV (Lang et al., 2011). The potential dependence of SARS-CoV-2 on HS for attachment and entry combined with antiviral data from other viruses suggest that negatively charged astodrimer sodium may have antiviral activity against SARS-CoV-2 *in vitro* by blocking the early virus-receptor recognition events.

Astodrimer sodium is a polyanionic dendrimer reformulated for use as a topical, nasally administered antiviral agent to inactivate SARS-CoV-2 before infection can occur. The potential advantages of astodrimer sodium over other technologies include its lack of systemic absorption following topical application (Chen et al., 2009; O'Loughlin et al., 2010; McGowan et al., 2011). In addition, the SI of astodrimer sodium for SARS-CoV-2 is high and in a vaginal gel formulation (10 mg/mL), the compound has been shown to be safe and effective in phase 2 and

large phase 3 trials for treatment and prevention of BV (Chavoustie et al., 2020; Waldbaum et al., 2020; Schwebke et al., 2021) and is now marketed in Europe, Australia, New Zealand and several countries in Asia. Astodrimer sodium is also the active antiviral substance in VivaGel® condom products that have marketing authorization in Europe, Japan, Australia/New Zealand and Canada. However, these current formulations are not appropriate for use to protect the respiratory tract from SARS-CoV-2 infection.

5. Conclusions

Data from the current studies, taken together with studies of astodrimer sodium antiviral activity against HIV-1, and HSV-1 and -2, indicate that the compound exerts its antiviral activity against geographically diverse SARS-CoV-2 isolates by interfering with the early virus-cell recognition events. Astodrimer sodium is a potent virucidal agent that reduces the infectivity of SARS-CoV-2 by >99.9% after 1 minute of exposure to the virus. These studies support astodrimer sodium being able to prevent early virus entry steps such as attachment, thereby reducing or preventing viral infection or cell-cell spread.

An antiviral agent such as astodrimer sodium that blocks binding of the virus to target cells could potentially be used as a preventive and/or a therapeutic agent against SARS-CoV-2. These antiviral studies suggest that reformulation of astodrimer sodium for delivery to the respiratory tract may be an effective preventive strategy to block SARS-CoV-2 transmission and augment other protective and therapeutic strategies.

The potent antiviral and virucidal activity of astodrimer sodium against SARS-CoV-2 warrants further investigation.

Tables

Table 1: Antiviral efficacy, measured by a reduction in CPE in virus-infected cells at Day 4 post-infection, and selectivity of astodrimer sodium against SARS-CoV-2 (hCoV-19/Australia/VIC01/2020) infection of Vero E6 cells

Compound / Assay Type	Repeat	EC_{50} (mg/mL)	CC_{50} (mg/mL)	SI
Astodrimer sodium added 1-hour pre-infection	Assay 1	0.004	2.93	793
	Assay 2	0.012	>0.863	>70
	Mean ± SD	0.008 ± 0.006	NC	>431[a]
Astodrimer sodium added 1-hour post-infection	Assay 1	0.002	3.29	2197
	Assay 2	0.011	>0.863	>80
	Mean ± SD	0.006 ± 0.007	NC	>1138[a]
Remdesivir added 1-hour post-infection	Assay 1	0.59 µM	>20 µM	>33
	Assay 2	0.61 µM	>20 µM	>33

EC_{50}=50% effective concentration; CC_{50}=50% cytotoxic concentration; SI=selectivity index (CC_{50}/EC_{50});
SD=standard deviation; NC=not calculated
[a] Average of Assay 1 and Assay 2 SI

Table 2: Antiviral efficacy, measured by a reduction in mean infectious virus (Log_{10} pfu/mL), and selectivity of astodrimer sodium against SARS-CoV-2 (2019-nCoV/USA-WA1/2020) on Day 4 post-infection

Compound / Assay Type	Cell Line	EC_{50} (mg/mL)	CC_{50} (mg/mL)	SI
Astodrimer sodium added 1-hour pre-infection	Vero E6	0.032	15.09	472
	Calu-3	0.037	21.76	588
Astodrimer sodium added at time of infection	Vero E6	0.020	15.09	755
	Calu-3	0.035	21.76	622
Astodrimer sodium added 1-hour post-infection	Vero E6	0.019	15.09	794
	Calu-3	0.030	21.76	725
Remdesivir added 1-hour post-infection	Vero E6	0.791 µM	N/A	N/A
	Calu-3	0.589 µM	N/A	N/A

EC_{50}=50% effective concentration; CC_{50}=50% cytotoxic concentration; SI=selectivity index (CC_{50}/EC_{50}); N/A=not applicable

Table 3: Virucidal efficacy of 10 mg/mL astodrimer sodium against SARS-CoV-2 (2019-nCoV/USA-WA1/2020), measured by a reduction in mean infectious virus (Log_{10} pfu/mL), at 96 hours post-infection

Viral Load (pfu/mL)	Virus:Astodrimer Incubation Time	Reduction vs. Virus Control (Log_{10} ± SD)	Reduction vs. Virus Control (%)
10^6	5 sec	0.10 ± 0.20	20.567
	10 sec	0.03 ± 0.06	7.388
	30 sec	0.10 ± 0.10	20.567
	1 min	0.33 ± 0.12	53.584
	10 min	2.20 ± 0.10	99.369
	15 min	3.67 ± 0.23	99.979
10^5	5 sec	0.33 ± 0.21	53.584
	10 sec	0.23 ± 0.06	41.566
	30 sec	0.30 ± 0.17	49.881
	1 min	0.47 ± 0.21	65.855
	10 min	3.70 ± 0.26	99.980
	15 min	4.60 ± 0.10	99.998
10^4	5 sec	-0.13 ± 0.21	-35.936
	10 sec	0.07 ± 0.29	14.230
	30 sec	0.10 ± 0.10	20.567
	1 min	0.10 ± 0.00	20.567
	10 min	5.07 ± 0.25	>99.999
	15 min	5.83 ± 0.12	>99.999

Shading indicates data points where virucidal efficacy is >99.9% (3 log_{10} reduction) vs. virus control; virus control=untreated virus, 0 mg/mL astodrimer sodium; SD=standard deviation

Table 4: Virucidal efficacy of 10 mg/mL astodrimer sodium against SARS-CoV-2 (2019-nCoV/USA-WA1/2020), measured by a reduction in mean infectious virus (Log_{10} pfu/mL), at 16 hours post-infection

Viral Load (pfu/mL)	Virus:Astodrimer Incubation Time	Reduction vs. Virus Control (Log_{10} ± SD)	Reduction vs. Virus Control (%)
10^5	30 sec	0.00 ± 0.36	0.000
	1 min	2.63 ± 0.15	99.767
	5 min	4.63 ± 0.31	99.998
	15 min	4.60 ± 0.10	99.998
10^4	30 sec	0.20 ± 0.20	36.904
	1 min	3.17 ± 0.12	99.932
	5 min	3.67 ± 0.21	99.979
	15 min	4.00 ± 0.10	99.990

Shading indicates data points where virucidal efficacy is >99.9% (3 log_{10} reduction) vs. virus control; virus control=untreated virus, 0 mg/mL astodrimer sodium
SD=standard deviation

Figure Captions

Figure 1. Dose-response and cytotoxicity analysis of SARS-CoV-2 (2019-nCoV/USA-WA1/2020) antiviral activity of astodrimer sodium in Vero E6 cells as measured by infectious virus release (Log_{10} pfu/mL) on Day 4 post-infection

Astodrimer sodium (0.0005 to 10 mg/mL) was added to cell cultures 1 hour prior to (t = -1h), at the time of (t = 0), and 1 hour post-infection (t = +1h). Cytotoxicity was assessed by LDH detection (OD @ 490 nm), with 0.5% saponin used as the positive cytotoxic control. Points and error bars represent mean ± SD of triplicate readings.

Figure 2. Dose-response and cytotoxicity analysis of SARS-CoV-2 (2019-nCoV/USA-WA1/2020) antiviral activity of astodrimer sodium in Calu-3 cells as measured by infectious virus release (Log_{10} pfu/mL) on Day 4 post-infection

Astodrimer sodium (0.0005 to 10 mg/mL) was added to cell cultures 1 hour prior to (t = -1h), at the time of (t = 0), and 1 hour post-infection (t = +1h). Cytotoxicity was assessed by LDH detection (OD @ 490 nm), with 0.5% saponin used as the positive cytotoxic control. Points and error bars represent mean ± SD of triplicate readings.

Figure 3. Virucidal efficacy of astodrimer sodium against SARS-CoV-2 (2019-nCoV/USA-WA1/2020) measured by a reduction in mean infectious virus (Log_{10} pfu/mL), at 96 hours post-infection in Vero E6 cells

Astodrimer sodium (1 to 30 mg/mL) was incubated with SARS-CoV-2 (2019-nCoV/USA-WA1/2020) for 5 sec up to 15 min. Treated virus was added to Vero E6 cells and the amount of infectious virus in the supernatant was determined by plaque assay 96 hours post-infection.

Graph shows dose-response of astodrimer sodium virucidal activity using 10^4 pfu/mL virus inoculum. Points and error bars represent mean ± SD of triplicate readings. Dotted line indicates level of mean infectious virus when untreated virus was added to Vero E6 cells (virus control).

Figure 4. Virucidal efficacy of astodrimer sodium against SARS-CoV-2 (2019-nCoV/USA-WA1/2020) measured by a reduction in mean infectious virus (Log_{10} pfu/mL), at 16 hours post-infection in Vero E6 cells

Astodrimer sodium (0.0046 to 30 mg/mL) was incubated with SARS-CoV-2 (2019-nCoV/USA-WA1/2020) for 30 sec, 1 min, 5 min and 15 min. Treated virus was added to Vero E6 cells and the amount of infectious virus in the supernatant was determined by plaque assay 16 hours post-infection. Graph shows dose-response of astodrimer sodium virucidal activity using 10^4 pfu/mL virus inoculum. Points and error bars represent mean ± SD of triplicate readings. Dotted line indicates level of mean infectious virus when untreated virus was added to Vero E6 cells (virus control).

Figure 5. Antiviral efficacy of astodrimer sodium and iota-carrageenan against SARS-CoV-2 (2019-nCoV/USA-WA1/2020) measured by a reduction in nucleocapsid (ng/mL), at Day 4 post-infection in human bronchial epithelial primary cells (HBEpC)

Astodrimer sodium (0, 1.1, 3.3 and 10 mg/mL) or iota-carrageenan (0, 6, 60 and 600 µg/mL) were added to cell cultures 1 hour prior to infection.

A. Dose-response of astodrimer sodium antiviral activity. Points and error bars represent mean ± SD of triplicate readings.

B. Dose-response of carrageenan antiviral activity. Points represent one replicate.

Dotted lines indicates level of inhibition achieved with positive control, SARS-CoV-2 pAb.

406 **Fig. 1**

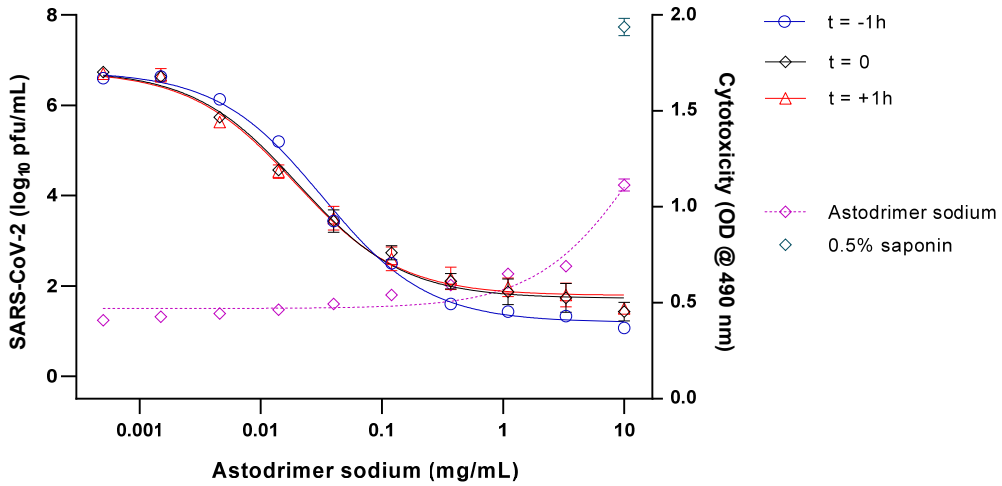

407

408 **Fig. 2**

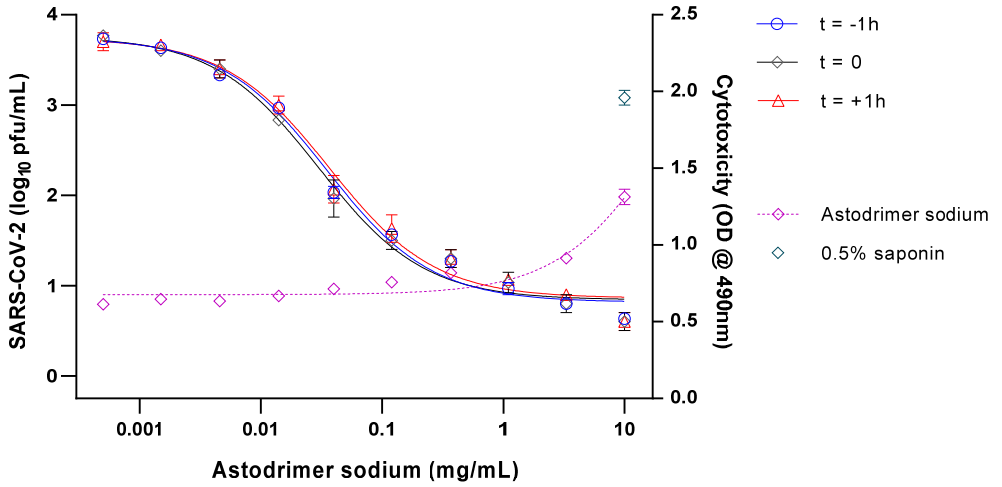

409

410

411 **Fig 3.**

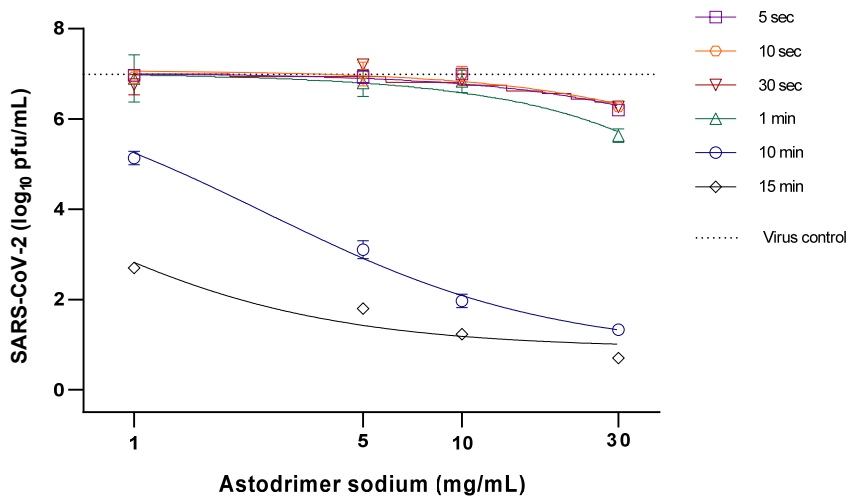

412

413 **Fig 4.**

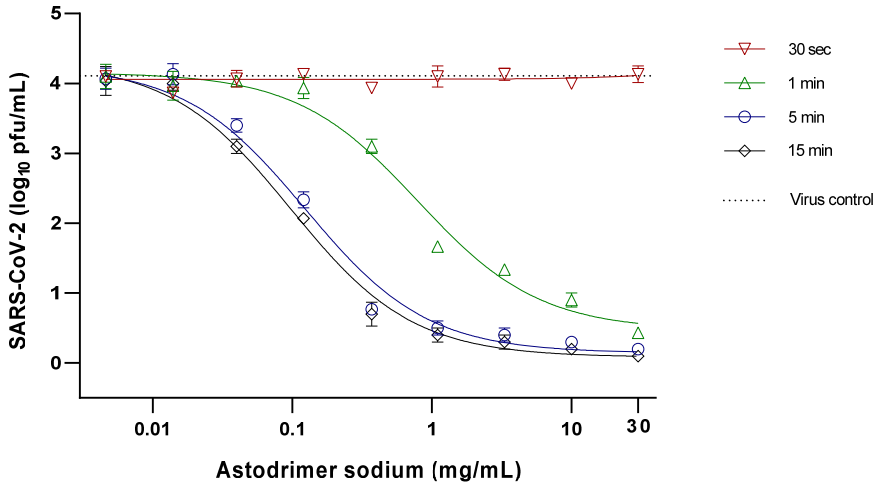

414

415

Fig 5.

A

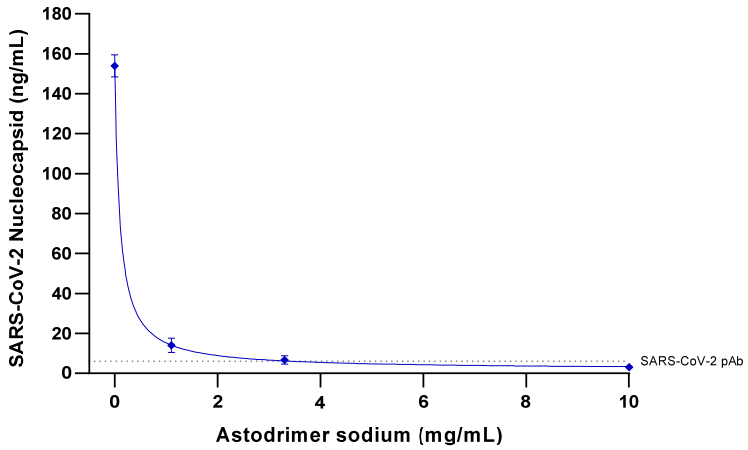
SARS-CoV-2 Nucleocapsid (ng/mL)
180
160
140
120
100
80
60
40
20
0
0
2
4
6
8
10
Astodrimer sodium (mg/mL)
SARS-CoV-2 pAb

B

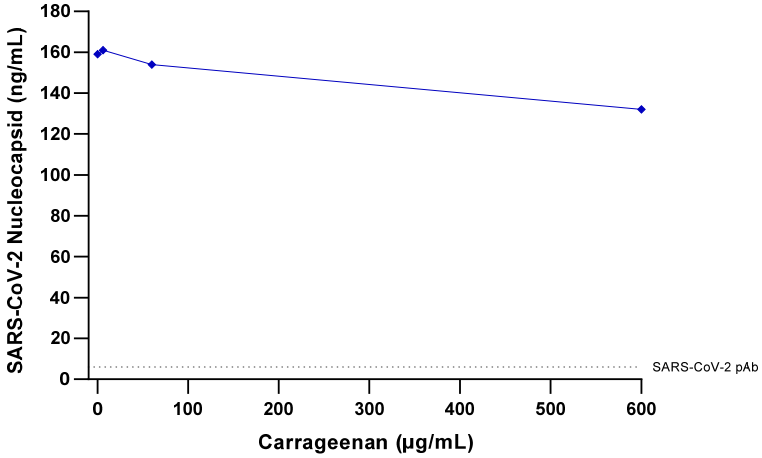
SARS-CoV-2 Nucleocapsid (ng/mL)
180
160
140
120
100
80
60
40
20
0
0
100
200
300
400
500
600
Carrageenan (µg/mL)
SARS-CoV-2 pAb

423

ACE2	angiotensin converting enzyme 2	LLOD	lower limit of detection
BSA	bovine serum albumin	MEM	minimal essential medium
BV	bacterial vaginosis	MOI	multiplicity of infection
CC_{50}	50% cytotoxic concentration	MTT	methylthiazolyldiphenyl-tetrazolium bromide
COVID-19	coronavirus disease 2019	NC	not calculated
CPE	cytopathic effect	OD	optical density
EC_{50}	50% effective concentration	pfu	plaque forming unit
ELISA	enzyme-linked immunosorbent assay	RBD	receptor binding domain
FBS	fetal bovine serum	S protein	spike protein
HBEpC	human bronchial epithelial primary cells	SARS-CoV	severe acute respiratory syndrome coronavirus
HIV-1	human immunodeficiency virus type 1	SARS-CoV-2	severe acute respiratory syndrome coronavirus 2
HPV	human papillomavirus	SD	standard deviation
HRSV	human respiratory syncytial virus	SHIV	simian-human immunodeficiency virus
HS	heparan sulfate proteoglycan	SI	selectivity index
HSV	herpes simplex virus	$TCID_{50}$	median tissue culture infective dose
HTEpC	human tracheal epithelial primary cells	TOA	time of addition

ITS	insulin-transferrin-selenium	TPCK	L-(tosylamido-2-phenyl) ethyl chloromethyl ketone
LDH	lactate dehydrogenase	UPLC	ultra-high-performance liquid chromatography

Acknowledgments

The authors were fully responsible for the content, editorial decisions, and opinions expressed in the current article. The authors would like to acknowledge 360Biolabs Pty Ltd (Melbourne, Australia) for the conduct of the CPE assays and Scripps Research Institute for the conduct of the antiviral and virucidal assays. The authors would also like to thank the Peter Doherty Institute for Infection and Immunity (Melbourne, Australia) for the gift to 360Biolabs of SARS-CoV-2 hCoV-19/Australia/VIC01/2020 used in these studies.

Funding

The research was funded by Starpharma Pty Ltd, which was responsible for study design, interpretation of data, writing the manuscript and decision to submit the article for publication.

References

Bernstein, D.I., Stanberry, L.R., Sacks, S., Ayisi, N.K., Gong, Y.H., Ireland, J., Mumper, R.J., Holan, G., Matthews, B, McCarthy, T., Bourne, N., 2003. Evaluations of unformulated and formulated dendrimer-based microbicide candidates in mouse and guinea pig models of genital herpes. Antimicrob. Agents Chemother. 47(12), 3784-3788. https://doi.org/10.1128/aac.47.12.3784-3788.2003

441 Bansal, S., Jonsson, C.B., Taylor, S.L., Figueroa, J.M., Vanesa, A.D., Palacios, C., Vega, J.C.,
442 2020. Iota-carrageenan and xylitol inhibit SARS-CoV-2 in cell culture. bioRxiv
443 2020.08.19.225854. https://doi.org/10.1101/2020.08.19.225854

444 Chavoustie, S.E., Carter, B.A., Waldbaum, A.S., Donders, G.G.G., Peters, K.H., Schwebke, J.R.,
445 Paull, J.R.A, Price, C.F., Castellarnau, A., McCloud, P., Kinghorn, G.R., 2020. Two phase
446 3, double-blinded, placebo-controlled studies of the efficacy and safety of Astodrimer 1%
447 Gel for the treatment of bacterial vaginosis. Eur. J. Obstet. Gynecol. Reprod. Biol. 245, 13-
448 18. https://doi.org/10.1016/j.ejogrb.2019.11.032

449 Chen, M.Y., Millwood, I.Y., Wand, H., Poynten, M, Law, M., Kaldor, J.M., Wesselingh, S.,
450 Price, C.F., Clark, L.J., Paull, J.R., Fairley, C.K., 2009. A randomized controlled trial of
451 the safety of candidate microbicide SPL7013 gel when applied to the penis. J. Acquir.
452 Immune Defic. Syndr. 50(4), 375-380. https://doi.org/10.1097/QAI.0b013e318198a7e6

453 Connell, B.J., Lortat-Jacob, H., 2013. Human immunodeficiency virus and heparan sulfate: from
454 attachment to entry inhibition. Frontiers Immunol. 4, 385.
455 https://doi.org/10.3389/fimmu.2013.00385

456 Ghosh, T., Chattopadhyay, K., Marschall, M., Karmakar, P., Mandal, P., Ray, B., 2009. Focus on
457 antivirally active sulfated polysaccharides: from structure-activity analysis to clinical
458 evaluation. Glycobiology 19(1), 2-15. https://doi.org/10.1093/glycob/cwn092

459 Gong, E., Matthews, B., McCarthy, T., Chu, J., Holan, G., Raff, J., Sacks, S., 2005. Evaluation
460 of dendrimer SPL7013, a lead microbicide candidate against herpes simplex virus.
461 Antiviral Res. 68(3), 139-146. https://doi.org/10.1016/j.antiviral.2005.08.004

462 Hoffmann, M., Kleine-Weber, H., Pöhlmann, S., 2020a. A multibasic cleavage site in the spike
463 protein of SARS-CoV-2 is essential for infection of human lung cells. Molecular Cell
464 78(4), 779-784.e5. https://doi.org/10.1016/j.molcel.2020.04.022

465 Hoffmann, M., Kleine-Weber, H., Schroeder, S., Krüger, N., Herrler, T., Erichsen, S.,
466 Schiergens, T.S., Herrler, G., Wu, N.H., Nitsche, A., Müller, M.A., Drosten, C., Pöhlmann,
467 S., 2020b. SARS-CoV-2 cell entry depends on ACE2 and TMPRSS2 and is blocked by a
468 clinically proven protease inhibitor. Cell 181(2), 271-280.e8.
469 https://doi.org/10.1016/j.cell.2020.02.052

470 Hou, Y.J., Okuda, K., Edwards, C.E., et al. 2020. SARS-CoV-2 reverse genetics reveals a
471 variable infection gradient in the respiratory tract. Cell 182(2), 429-446.e14.
472 https://doi.org/10.1016/j.cell.2020.05.042

473 Jiang, Y.H., Emau, P., Cairns, S., Flanary, L., Morton, W.R., McCarthy, T., Tsai, C.C., 2005.
474 SPL7013 gel as a topical microbicide for prevention of vaginal transmission of $SHIV_{89.6P}$
475 in macaques. AIDS Res. Hum. Retroviruses 21(3), 207-213.
476 https://doi.org/10.1089/aid.2005.21.207

477 Korber, B., Fischer, W.M., Gnanakaran, S., Yoon, H., Theiler, J., Abfalterer, W., Foley, B.,
478 Giorgi, E.E., Bhattacharya, T., Parker, M.D., Partridge, D.G., Evans, C.M., de Silva, T.I.,
479 LaBranche, C.C., Montefiori, D.C., 2020. Spike mutation pipeline reveals the emergence
480 of a more transmissible form of SARS-CoV-2. bioRxiv.
481 https://doi.org/10.1101/2020.04.29.069054

482 Lackman-Smith, C., Osterling, C., Luckenbaugh, K., Mankowski, M., Snyder, B., Lewis, G.,
483 Paull, J., Profy, A., Ptak, R.G., Buckheit Jr., R.W., Watson, K.M., Cummins Jr., J.E.,
484 Sanders-Beer, B.E., 2008. Development of a comprehensive human immunodeficiency

485 virus type-1 screening algorithm for discovery and preclinical testing of topical
486 microbicides. Antimicrob. Agents Chemother. 52(5), 1768-1781.
487 https://doi.org/10.1128/AAC.01328-07

488 Lang, J., Yang, N., Deng, J., Liu, K., Yang, P., Zhang, G., Jiang, C., 2011. Inhibition of SARS
489 pseudovirus cell entry by lactoferrin binding to heparan sulfate proteoglycans. PLoS ONE
490 6(8), e23710. https://doi.org/10.1371/journal.pone.0023710

491 Liu, L., Chopra, P., Li, X., Wolfert, M.A., Tompkins, S.M., Boons, G.J., 2020. SARS-CoV-2
492 spike protein binds heparan sulfate in a length- and sequence-dependent manner. bioRxiv.
493 https://doi.org/10.1101/2020.05.10.087288

494 McCarthy, T.D., Karellas, P., Henderson, S.A., Giannis, M., O'Keefe, D.F., Heery, G., Paull,
495 J.R.A., Matthews, B.R., Holan, G., 2005. Dendrimers as drugs: discovery and preclinical
496 and clinical development of dendrimer microbicides for HIV and STI prevention. Mol.
497 Pharm. 2(4), 312-318. https://doi.org/10.1021/mp050023q

498 McGowan, I., Gomez, K., Bruder, K., Febo, I., Chen, B.A., Richardson, B.A., Husnik, M.,
499 Livant, E., Price, C., Jacobson, C., 2011. Phase 1 randomized trial of the vaginal safety and
500 acceptability of SPL7013 gel (VivaGel®) in sexually active young women (MTN-004).
501 AIDS 25(8), 1057-1064. https://doi.org/10.1097/QAD.0b013e328346bd3e

502 Milewska, A., Zarebski, M., Nowak, P., Stozek, K., Potempa, J., Pyrc, K., 2014. Human
503 coronavirus NL63 utilizes heparan sulfate proteoglycans for attachment to target cells. J.
504 Virol. 88(22), 13221-13230. https://doi.org/10.1128/JVI.02078-14

505 Mycroft-West, C., Su, D., Elli, S., Li, Y., Guimond, S., Miller, G., Turnbull, J., Yates, E.,
506 Guerrini, M., Fernig, D., Lima, M., Skidmore, M., 2020a. The 2019 coronavirus (SARS-

CoV-2) surface protein (spike) S1 receptor binding domain undergoes conformational change upon heparin binding. bioRxiv. https://doi.org/10.1101/2020.02.29.971093

Mycroft-West, C.J., Su, D., Li, Y., Guimond, S., Rudd, T.R., Elli, S., Miller, G., Nunes, Q.M., Procter, P., Bisio, A., Forsyth, N.R., Turnbull, J.E., Guerrini, M., Fernig, D., Yates, E.A., Lima, M.A., Skidmore, M.A., 2020b. SARS CoV-2 spike S1 receptor binding domain undergoes conformational change upon interaction with low molecular weight heparins. bioRxiv. https://doi.org/10.1101/2020.04.29.068486

Mycroft-West, C.J., Su, D., Pagani, I., Rudd, T.R., Elli, S., Guimond, S., Miller, G., Meneghetti, M.C.Z., Nader, H.B., Li, Y., Nunes, Q.M., Procter, P., Mancini, N., Clementi, M., Forsyth, N.R., Turnbull, J.E., Guerrini, M., Fernig, D., Vicenzi, E., Yates, E.A., Lima, M.A., Skidmore, M.A., 2020c. Heparin inhibits cellular invasion of SARS-CoV-2: structural dependence on the interaction of the surface protein (spike) S1 receptor binding domain with heparin. bioRxiv 2020.2004.2028.066761. https://doi.org/10.1101/2020.04.28.066761

O'Loughlin, J., Millwood, I.Y., McDonald, H.M., Price, C.F., Kaldor, J.M., Paull, J.R.A., 2010. Safety, tolerability, and pharmacokinetics of SPL7013 gel (VivaGel®): a dose ranging phase 1 study. Sex. Transm. Dis. 37(2), 100-104. https://doi.org/10.1097/OLQ.0b013e3181bc0aac

Ogando, N.S., Dalebout, T.J., Zevenhoven-Dobbe, J.C., Limpens, R.W.A.L., van der Meer, Y., Caly, L., Druce, J., de Vries, J.J.C., Kikkert, M., Bárcena, M., Sidorov, I., Snijder, J., 2020. SARS-coronavirus-2 replication in Vero E6 cells: replication kinetics, rapid adaption and cytopathology. J. General Virol. 10.1099/jgv.0.001453. Advance online publication. https://doi.org/10.1099/jgv.0.001453

529 Pauwels, R., Balzarini, J., Baba, M., Snoeck, R., Schols, D., Herdewijn, P., Desmyter, J., De
530 Clercq, E., 1988. Rapid and automated tetrazolium-based colorimetric assay for the
531 detection of anti-HIV compounds. J. Virol. Methods 20(4), 309-321.
532 https://doi.org/10.1016/0166-0934(88)90134-6

533 Pizzorno, A., Padey, B., Dubois, J., Julien, T., Traversier, A., Dulière, V., Brun, P., Lina, B.,
534 Rosa-Calatrava, M., Terrier, O., 2020. In vitro evaluation of antiviral activity of single and
535 combined repurposable drugs against SARS-CoV-2. Antiviral Res. 104878. Advance
536 online publication. https://doi.org/10.1016/j.antiviral.2020.104878

537 Qiao, B., Olvera de la Cruz, M., 2020. The distal polybasic cleavage sites of SARS-CoV-2 spike
538 protein enhance spike protein-ACE2 binding. bioRxiv June 10.
539 https://doi.org/10.1101/2020.06.09.142877

540 Sarrazin, S., Lamanna, W.C., Esko, J.D., 2011. Heparan sulfate proteoglycans. Cold Spring
541 Harb. Perspect. Biol. 3(7), a004952. https://doi.org/10.1101/cshperspect.a004952

542 Schwebke, J., Carter, B., Waldbaum, A., Price, C., Castellarnau, A., Paull, J., McCloud, P.,
543 Kinghorn, G., 2021. A phase 3, randomized, controlled trial of Astodrimer 1% Gel for
544 preventing recurrent bacterial vaginosis. Eur. J. Obstet. Gynecol. Reprod. Biol. X 10,
545 100121. https://doi.org/10.1016/j.eurox.2021.100121

546 Sungnak, W., Huang, N., Bécavin, C., Berg, M., Queen, R., Litvinukova, M., Talavera-López,
547 C., Maatz, H., Reichart, D., Sampaziotis, F., Worlock, K.B., Yoshida, M., Barnes, J.L.,
548 2020. SARS-CoV-2 entry factors are highly expressed in nasal epithelial cells together
549 with innate immune genes. Nat. Med. 26(5), 681-687. https://doi.org/10.1038/s41591-020-
550 0868-6

551 Telwatte, S., Moore, K., Johnson, A., Tyssen, D., Sterjovski, J., Aldunate, M., Gorry, P.R.,
552 Ramsland, P.A., Lewis, G.R., Paull, J.R.A., Sonza, S., Tachedjian, G., 2011. Virucidal
553 activity of the dendrimer microbicide SPL7013 against HIV-1. Antiviral Res. 90(3), 195-
554 199. https://doi.org/10.1016/j.antiviral.2011.03.186

555 Tyssen, D., Henderson, S.A., Johnson, A., Sterjovski, J, Moore, K., La, J., Zanin, M., Sonza, S.,
556 Karellas, P., Giannis, M.P., Krippner, G., Wesselingh, S., McCarthy, T., Gorry, P.R.,
557 Ramsland, P.A., Cone, R., Paull, J.R.A., Lewis, G.R., Tachedjian, G., 2010. Structure
558 activity relationship of dendrimer microbicides with dual action antiviral activity. PLoS
559 ONE 5(8), e12309. https://doi.org/10.1371/journal.pone.0012309

560 van den Worm, S.H., Eriksson, K.K., Zevenhoven, J.C., Weber, F., Zust, R., Kuri, T., Dijkman,
561 R., Chang, G., Siddell, S.G., Snijder, E., Thiel, V., Davidson, A.D., 2012. Reverse genetics
562 of SARS-related coronavirus using vaccinia virus-based recombination. PLoS ONE
563 7(3):e32857. https://doi.org/10.1371/journal.pone.0032857

564 Waldbaum, A.S., Schwebke, J.R., Paull, J.R.A., Price, C.F., Edmondson, S.R., Castellarnau, A.,
565 McCloud, P., Kinghorn, G.R., 2020. A phase 2, double-blind, multicenter, randomized,
566 placebo-controlled, dose-ranging study of the efficacy and safety of Astodrimer Gel for the
567 treatment of bacterial vaginosis. PLoS ONE 15(5), e0232394.
568 https://doi.org/10.1371/journal.pone.0232394

569 Walls, A.C., Park, Y.J., Tortorici, M.A., Wall, A., McGuire, A.T., Veesler, D., 2020. Structure,
570 function and antigenicity of the SARS-CoV-2 spike glycoprotein. Cell 181(2), 281-292.e6
571 https://doi.org/10.1016/j.cell.2020.02.058

572 Wang, M., Cao, R., Zhang, L., Yang, X., Liu, J., Xu, M/., Shi, Z., Hu, Z., Zhong, W., Xiao, G.,
573 2020. Remdesivir and chloroquine effectively inhibit the recently emerged novel
574 coronavirus (2019-nCoV) in vitro. Cell Res. 30(3), 269-271.
575 https://doi.org/10.1038/s41422-020-0282-0

576 Wrapp, D., Wang, N., Corbett, K.S., Goldsmith, J.A., Hsieh, C.L., Abiona, O., Graham, B.S.,
577 McLellan, J.S., 2020. Cryo-EM structure of the 2019-nCoV spike in the prefusion
578 conformation. Science 367(6483), 1260-1263. https://doi.org/10.1126/science.abb2507

579 Yuan, M., Wu, N.C., Zhu, X., Lee, C.C.D., So, R.T.Y., Lv, H., Mok, C.K.P., Wilson, I.A., 2020.
580 A highly conserved cryptic epitope in the receptor binding domains of SARS-CoV-2 and
581 SARS-CoV. Science 368(6491), 630-633. https://doi.org/10.1126/science.abb7269

582

Figures

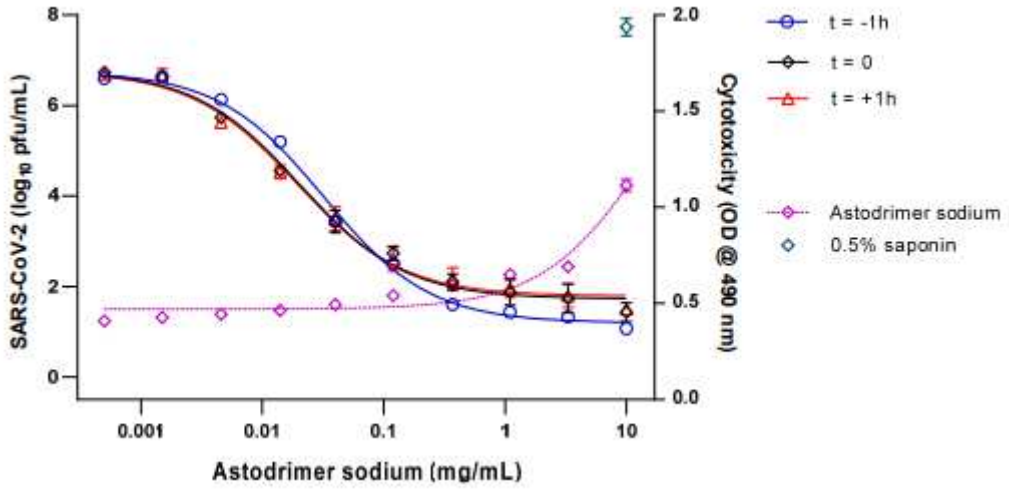

Figure 1

Dose-response and cytotoxicity analysis of SARS-CoV-2 (2019-nCoV/USA WA1/2020) antiviral activity of astodrimer sodium in Vero E6 cells as measured by infectious virus release (Log10 pfu/mL) on Day 4 post-infection

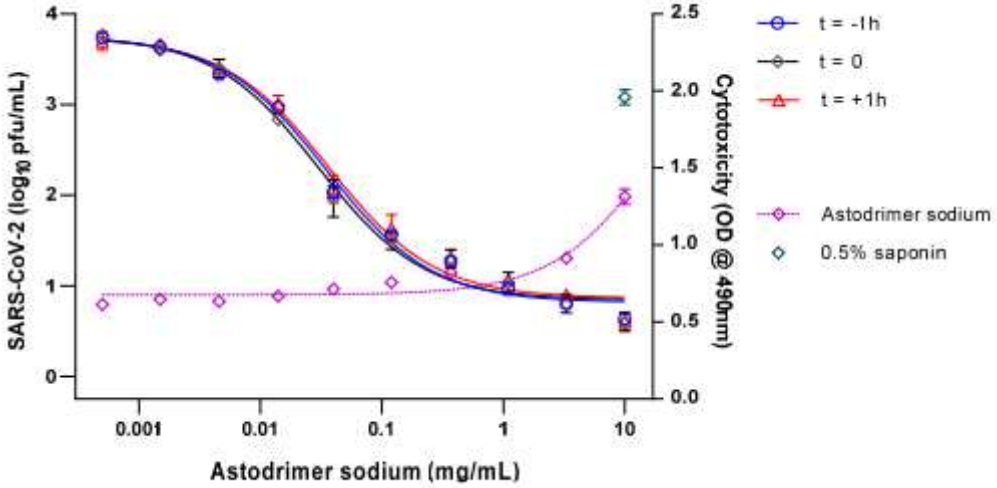

Figure 2

Dose-response and cytotoxicity analysis of SARS-CoV-2 (2019-nCoV/USA WA1/2020) antiviral activity of astodrimer sodium in Calu-3 cells as measured by infectious virus release (Log10 pfu/mL) on Day 4 post-infection

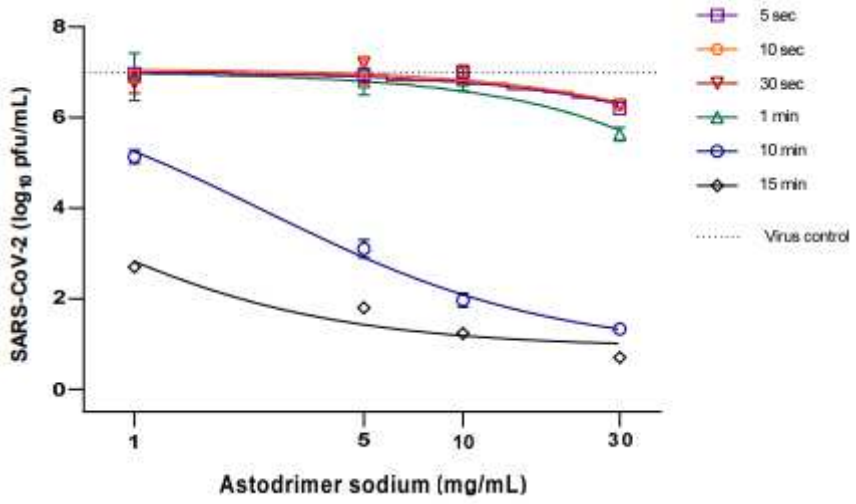

Figure 3

Virucidal efficacy of astodrimer sodium against SARS-CoV-2 (2019-nCoV/USA WA1/2020) measured by a reduction in mean infectious virus (Log10 pfu/mL), at 96 hours post-infection in Vero E6 cells

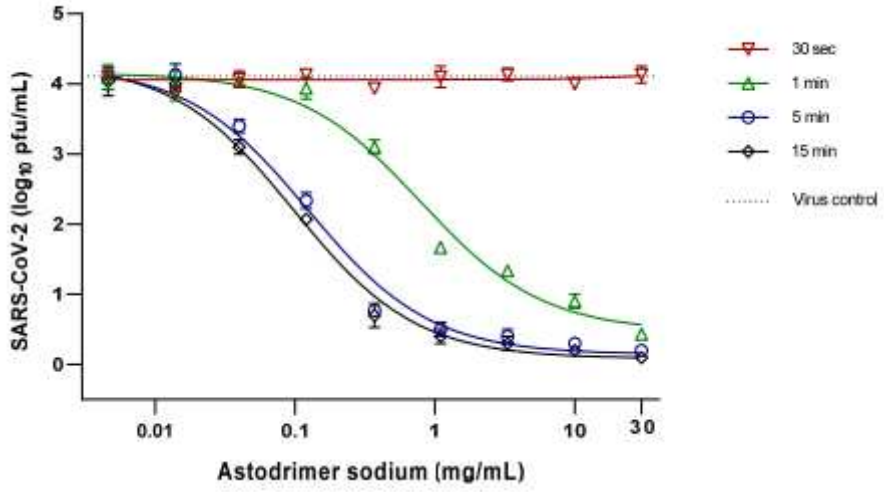

Figure 4

Virucidal efficacy of astodrimer sodium against SARS-CoV-2 (2019-nCoV/USA WA1/2020) measured by a reduction in mean infectious virus (Log10 pfu/mL), at 16 hours post-infection in Vero E6 cells

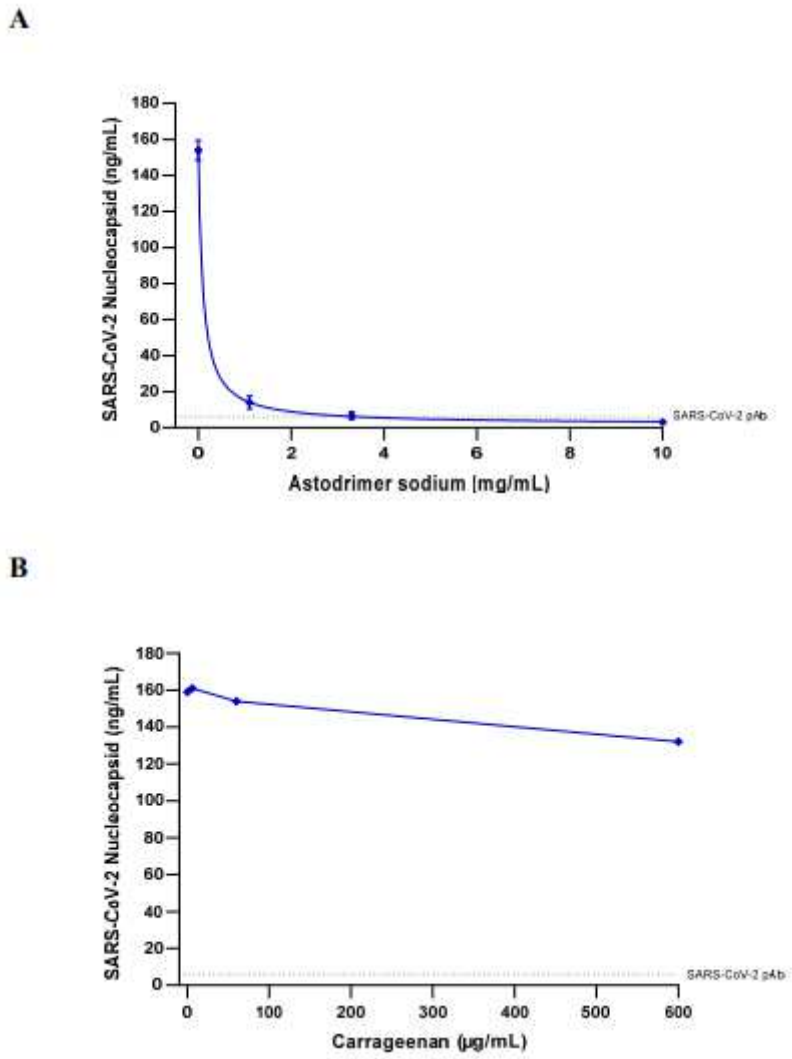

Figure 5

Antiviral efficacy of astodrimer sodium and iota-carrageenan against SARS CoV-2 (2019-nCoV/USA-WA1/2020) measured by a reduction in nucleocapsid (ng/mL), at Day 4 post-infection in human bronchial epithelial primary cells (HBEpC)